

# AI-driven remote sensing enhances Mediterranean seagrass monitoring and conservation to combat climate change and anthropogenic impacts

**Masuma Chowdhury**

`masuma.chowdhury@quasarsr.com`

Quasar Science Resources, S.L.

**Alejo Martínez-Sansigre**

Quasar Science Resources, S.L.

**Maruška Mole**

Quasar Science Resources, S.L.

**Eduardo Alonso Peleato**

Quasar Science Resources, S.L.

**Nadiia Basos**

Quasar Science Resources, S.L.

**Jose Manuel Blanco**

Quasar Science Resources, S.L.

**Maria Ramirez**

Quasar Science Resources, S.L.

**Isabel Caballero**

Institute of Marine Sciences of Andalusia, Spanish National Research Council (ICMAN-CSIC)

**Ignacio de la Calle**

Quasar Science Resources, S.L.

---

## Article

### Keywords:

**Posted Date:** September 15th, 2023

**DOI:** <https://doi.org/10.21203/rs.3.rs-3304270/v1>

**License:**   This work is licensed under a Creative Commons Attribution 4.0 International License.

[Read Full License](#)

**Additional Declarations:** No competing interests reported.

---

**Version of Record:** A version of this preprint was published at Scientific Reports on April 10th, 2024. See the published version at <https://doi.org/10.1038/s41598-024-59091-7>.

# Abstract

Seagrasses are undergoing widespread loss due to anthropogenic pressure and climate change. Since 1960, the Mediterranean seascape lost 13–50% of the areal extent of its dominant and endemic seagrass- *Posidonia oceanica*, which regulates its ecosystem. Many conservation and restoration projects failed due to poor site selection and lack of long-term monitoring. Here, we present a fast and efficient operational approach based on a deep-learning artificial intelligence model using Sentinel-2 data to map the spatial extent of the meadows, enabling short and long-term monitoring, and identifying the impacts of natural and human-induced stressors and changes at different timescales. We apply ACOLITE atmospheric correction to the satellite data and use the output to train the model along with the ancillary data and map the extent of the meadows. We apply noise-removing filters to enhance the map quality. We obtain 74–92% of overall accuracy, 72–91% of user's accuracy, and 81–92% of producer's accuracy, where high accuracies are observed at 0-25m depth. Our model is easily adaptable to other regions and can produce maps in *in-situ* data-scarce regions, providing a first-hand overview. Our approach can help restoration practitioners, conservationists and ecosystem managers to make rational decisions to protect this species and promote sustainability.

## Introduction

Seagrasses, the submersed marine flowering plants, are undergoing substantial decline due to direct and indirect anthropogenic activities and climate change. The recent publication<sup>1</sup> estimated the global seagrass area to date as 160,387 to 266,562 square km, which is significantly lower than the previously reported global seagrass spatial distribution ranging from 177,000 to 600,000 square km<sup>2,3</sup>. Their loss rates accelerate from 0.9% yr<sup>-1</sup> in the 1940s to 7% yr<sup>-1</sup> toward the end of the 20th century, making them one of the most threatened ecosystems on Earth<sup>4,5</sup>. Since 1960, the Mediterranean seascape lost 13–50% of the areal extent of its most common and endemic *Posidonia oceanica* seagrass meadows<sup>6</sup>. If the recent heat waves in the Mediterranean Sea continues, this seagrass may disappear within 100 to 150 years<sup>7</sup>. Recently, efforts to protect *P. oceanica* have led to the creation of the *Mediterranean Posidonia Network (MPN)* (<https://medposidonianetwork.com/>) including more than 50 stakeholders from 10 countries, which seeks to effectively protect 100% of *P. oceanica* by 2030 by introducing innovative tools and raising awareness at the local, national, and international levels about the importance of this species<sup>8</sup>. However, the lack of a multi-temporal monitoring system over large areas, and identifying the hotspot to mitigate the rapid degradation caused by anthropogenic pressures are becoming a major concern for Mediterranean coastal managers, affecting the conservation program to protect this species.

*P. oceanica* covers 50,000 square km of coastal sandy and rocky areas consisting of 25% of the Mediterranean Sea bottom at 0 to 40 m depth<sup>9,10</sup>. The meadows are home to about 20% of Mediterranean sea life species and can accommodate up to 350 animal species per hectare<sup>11–13</sup>. They contribute to different coastal processes like sediment deposition, and attenuate currents and wave energy<sup>14</sup>. They are globally significant carbon sinks with greater organic carbon density compared to

estuarine mangroves, peatlands and tropical forests<sup>15,16</sup>, thus play a key role in climate change mitigation<sup>17</sup>. However, the meadows are susceptible to increasing heat waves and climate change<sup>18–20</sup>. Besides, the meadows are under substantial threat by different anthropogenic activities, i.e., 22% of construction of coastal infrastructure, 23% of water pollution, 14% of invasive species, 18% of Fishing, 5% of shipping and 18% of modifications of marine currents and hydrography<sup>21</sup> (Fig. 1). The European Union (EU) Habitats Directive 92/43/EEC has listed *P. oceanica* meadows as a priority habitat. *P. oceanica* is also a protected species in the Natura2000 networks within the EU because of its significant influences on the surrounding biological, biogeochemical and physical processes in the littoral<sup>22</sup>.

A successful conservation programme for *P. oceanica* involves knowledge about the spatial extent of the meadows, understanding processes of degradation<sup>23</sup>; identifying causes of degradation<sup>24</sup>; designing and implementing effective monitoring programmes to manage, restore, or create these seagrass meadows<sup>25,26</sup>. This demands fast, cost-effective and validated methods to observe and monitor the present state, spatial pattern, and dynamics at appropriate spatial and temporal scales<sup>27,28</sup>. Multiple studies<sup>29–38</sup> presented the potential of remote sensing data in mapping the extent of this seagrass species, complementing the traditional *in-situ* monitoring system. However, they were mostly for proof of concept to utilize satellite-derived data and hardly capable of supporting the continuous monitoring system since they are computationally expensive, and require validated methods that can map across large areas with adequate accuracy and precision.

With growing archives of freely accessible earth observation data of adequate spatial and temporal resolution, along with fast-growing computational processing capabilities, we now have the potential tools to support mapping and monitoring of *P. oceanica* over large regions. To our knowledge, there is no use of remote sensing techniques coupled with deep-learning-based artificial intelligence, integrated within a pipeline technique that facilitates reproducibility and scalability to monitor the multi-temporal spatial extent of this seagrass species, thus supporting the conservation activity. In this study, we present an operational approach aiming to fill this gap. Our approach corresponds to a Scientific Exploitation Platform (SEP) dedicated to the extraction and processing of Earth observation (EO) products by adding one more layer on top of the existing tools to take the exploitation of the raw satellite data one step further. The proposed pipeline used Sentinel-2 data for the artificial intelligence deep-learning neural network (DLNN) to produce multi-temporal maps of *P. oceanica*. Here, we present the results for four major islands of the Balearic Islands, i.e. Menorca, Mallorca, Ibiza, and Formentera in Spain, and the Maltese Islands (Fig. 2). For these regions, we have trained the DLNN model and evaluated its performance under the scheme of long-term monitoring and evaluation to support conservation and ecosystem management to minimize climate change and anthropogenic impacts. This study should be of interest to scientists, conservationists and/or coastal managers, who are responsible for the challenging short-term management and long-term policy decisions to protect this type of natural resources.

## Results and Discussion

Maps of *P. oceanica*

We have detected 577.29 and 74.27 square km of *P. oceanica* respectively in the Balearic Islands and the Maltese Islands during 2021 (Fig. 3). Our proposed method is based on pixel-by-pixel classification schemes, and the final output map has 10m spatial resolution. We have stacked 3–9 atmospherically corrected clear Sentinel-2 level-2 images per tile (Supplementary Table S1) and applied the DLNN model with the corresponding *in-situ* and bathymetry data. The yearly stacked image reduced the potential misclassification due to non-persistent and seasonal variations in algal growth that may have similar signals. It was evident that depending on the region, our proposed approach was capable of mapping *P. oceanica* with 74–92% of overall accuracy, 72–91% of user’s accuracy, and 81–92% producer’s accuracy (Table 1). When a satellite pixel contained a region with sparsely distributed or unhealthy *P. oceanica* (according to the *in-situ* data), it was classified as false negative (FN) due to weak spectral signal. In contrast, when majority parts of the pixel contained healthy *P. oceanica*, it was classified as false positives (FP) due to strong spectral signal. However, in the north and northeast parts of Ibiza, we have observed swell noise in all the available Sentinel-2 images that caused residual noise in the yearly stacked image and resulted in misclassification. In contrast, we have noticed a different scenario in Malta. In the southeastern part of Malta, we observed the presence of spectral signals coming through the water column, which were identified by the DLNN model as *P. oceanica*. In this context, there could be two possible explanations, i.e., incomplete *in-situ* database, where the identified patches of *P. oceanica* were not included; consequently, it was depicted as FP during accuracy assessment; or, the presence of another seagrass species with similar signals. It should be noted that the *in-situ* data used in this study came from several years of field campaigns and might not be up-to-date in every region. As a result, in some places, the FP and FN identified in the final maps could be a true presentation of the current scenario and stressed the need for further investigation.

Table 1  
DLNN model performance in regional mapping of *P. oceanica* during 2021

| Location       | Overall Accuracy (%) | User’s accuracy (%) | Producer’s accuracy (%) |
|----------------|----------------------|---------------------|-------------------------|
| Formentera     | 92                   | 91                  | 91                      |
| Ibiza          | 78                   | 72                  | 88                      |
| Mallorca       | 88                   | 84                  | 81                      |
| Menorca        | 86                   | 83                  | 86                      |
| Maltese Island | 74                   | 74                  | 92                      |

Our model obtained a higher user’s and producer’s accuracy at 0-25m depth (Table 2), which was the most representative depth limit of the seabed detection using Sentinel-2 satellite in the Mediterranean Sea<sup>36,39</sup>. As the water was transparent and Sentinel-2 could see accurately enough, the model showed higher accuracy at this depth. With increasing depth and light attenuation, there could still be some *P.*

*oceanica* living on the sea bottom up to 40m depth<sup>40,41</sup> but the satellite could not see them accurately enough. This explained the model's performance with comparatively low accuracies at that depth.

Table 2  
DLNN model performance by depth in regional mapping of *P. oceanica* during 2021

|                         | Menorca   |            | Mallorca  |            | Ibiza     |            | Formentera |            | Maltese Islands |            |
|-------------------------|-----------|------------|-----------|------------|-----------|------------|------------|------------|-----------------|------------|
| Statistics<br>Depth     | 0-<br>25m | 25-<br>40m | 0-<br>25m | 25-<br>40m | 0-<br>25m | 25-<br>40m | 0-<br>25m  | 25-<br>40m | 0-<br>25m       | 25-<br>40m |
| Overall Accuracy (%)    | 86        | 86         | 86        | 90         | 85        | 70         | 93         | 90         | 77              | 71         |
| User's accuracy (%)     | 86        | 79         | 85        | 81         | 81        | 56         | 93         | 88         | 77              | 71         |
| Producer's accuracy (%) | 90        | 82         | 86        | 69         | 95        | 76         | 96         | 83         | 92              | 92         |

One of the advantages of our proposed method is the classification scheme. We trained the DLNN model to learn how the colour of the sea bottom with and without *P. oceanica* varied with depth. Besides, we designed the DLNN model for pixel-by-pixel classification per tile. As a result, our model was easily adaptable to other regions. We obtained accurate and reliable results while training the DLNN model with *in-situ* data from the target region, however, without *in-situ* data, the model was still capable of producing reliable maps which could provide a first-hand overview. To apprehend this, we reproduced the map of *P. oceanica* in the Maltese Island using the training dataset from Formentera (Fig. 4). The final output showed an overall accuracy of 64% with a user's accuracy of 73% and a producer's accuracy of 69%. As expected, the model performance was lower than what we observed in Table 1, however, it was still scientifically acceptable and could provide a general idea of the spatial extent of the meadows. It was evident that in both cases (Figs. 3i-j and 4) the model identified *P. oceanica* in the southeastern part of Malta, implying strong evidence of the presence of the seagrass meadows.

### Yearly monitoring of *P. oceanica* and its change assessment

We applied our proposed approach to perform a time-series analysis (Fig. 5 and Supplementary Table S2) in Formentera, as this region was highly renowned for conservation activities. While the seagrass patches mostly looked stable during 2017–2021, we detected changes in the northern and northeastern parts of Formentera. Especially, in the northern part of the island, we detected a loss of *P. oceanica* meadows until 2019 and then a subsequent gain after 2020. The change assessment between 2017 and 2021 showed that the area of the meadow increased by about 8 square km and decreased by about 1 square km, with a net gain of 7 square km, which might be a result of the current conservation activities. This showed the promising capabilities of our proposed approach to support monitoring of the meadows in the short and long term.

# Application in conservation and ecosystem management

In the recent past, the concept of natural recolonization (cutting and seedlings) has been introduced to restore *P. oceanica* meadows in the Mediterranean basin. However, most of them failed due to either choosing the wrong site where the species had never been before or a lack of long-term monitoring system due to economic constraints<sup>42</sup>. In addition, conservation and ecosystem management demand explicit and up-to-date knowledge to deal with real-time situations. Timely and reliable maps with a large spatial and temporal coverage can provide substantial ground in capacity building and making decisions. Unlike the available methodologies that were resource expensive and developed for a local scale, our proposed method can generate maps of *P. oceanica* with adequate accuracy in a cost-effective manner. This can add value to the current restoration programmes by identifying suitable sites and monitoring them regularly for short-term goals and long-term evaluation. Besides, the information generated through our approach can support conservationists and ecosystem managers in making rational decisions to promote sustainability.

In this context, we present an example in Fig. 6. The figure demonstrates boat pressure over the seagrass patches in Formentera and Ibiza during June-August 2021, a peak tourist season. Each hexagon mesh presents the number of ships detected using Sentinel-1 satellite data. It was evident that the channel between Formentera and Ibiza had the highest pressure within this period, thus showing the promising capabilities to identify the hotspot of *P. oceanica* for conservation and sustainable coastal resource management.

This study facilitates the continuous and long-term monitoring of *P. oceanica* in the Mediterranean Sea in an efficient manner. Our approach can be used in data-scarce region, with environmental and other constraints that make it impossible to collect in situ data, thus providing a first-hand overview. Besides, our approach can be a stepping-stone for recording the long-term impact of climate change as well as different environmental drivers and stressors on the seagrass meadows following a standardized and uniform method, and ameliorate understanding of the connectivity between oceanography and seagrass ecosystem, spatial and temporal management and protection, and finally mapping other benthic ecosystems for conservation and management.

## Methods

### Scientific exploitation platform

To map *P. oceanica* in a fast, reliable and efficient way, we developed an operational pipeline (Supplementary Figure S1) within a SEP. SEP integrated the hardware/software infrastructures that supplied the computing and storage resources needed for the exploitation and provision of the tools to manage EO datasets in a distributed environment. The platform comprised a Kubernetes cluster with many nodes hosted on-premises. The pipeline consisted of several scientific modules, such as data acquisition, data pre-processing, followed by artificial intelligence-based DLNN, and post-processing.

Within the SEP, all these modules could be executed isolated or sequentially within Docker containers, encapsulating the entire environment required for the scientific workflow. This ensured scalability and the pipeline's results could easily be reproduced with consistent outcomes. The pipeline also integrated a quality control system where a Network-file-system (NFS) volume held the raw data and the processed products, which could later be downloaded and analysed within the SEP web interface.

## Data acquisition

Sentinel-2 Level-1C data were downloaded from Google Cloud Storage using their Application Programming Interface (API). This data corresponded to the top of the atmospheric reflectance (TOA) for 7 Sentinel-2 tiles covering the Balearic Islands, and 1 tile covering the Maltese Islands (Supplementary Table S1). After visual inspection, images with high cloud coverage or sun glint effects were discarded from further processing. While mapping *P. oceanica*, bathymetry data plays a significant role, as this species is highly depth-dependent. In this study, the freely available bathymetry data at 100m spatial resolution were obtained from the European Marine Observation and Data Network (EMODnet, <https://www.emodnet-bathymetry.eu/>). Besides, the *in-situ* data were collected from the local government of the Balearic Islands and the Marine Database of Environment and Resources Authority (ERA) in Malta (<https://meps.eraportal.org.mt/>) to develop and train the DLNN model. These data corresponded to single cartography in the GIS layer combining several years of field campaigns during 2008–2019 for the Balearic Islands and 2017–2019 for the Maltese Islands. The data from the Balearic Islands (<https://atlasposidonia.com/en/home/>) had information for different marine habitats following the nomenclature and coding of the Standard List of Marine Habitats of Spain (LPHME), whereas the data from the Maltese Islands only had information regarding the habitat of *P. oceanica*.

## Data pre-processing

Pre-processing is a crucial step while producing benthic maps using satellite data for artificial intelligence. It is even more important while using Sentinel-2 data for aquatic applications as it has low-signal-to-noise-ratio that requires a good atmospheric correction (AC) to separate the top-of-atmospheric (TOA) reflectance observed by the satellite into the signal from the atmosphere and the signal from the surface (bottom-of-atmosphere, BOA)<sup>43</sup>. In this study, we applied the ACOLITE (v2020) AC processor developed by the Royal Belgian Institute of Natural Sciences (RBINS). Based on the literature and the analysis results, we chose ACOLITE because it better reproduced the shape of the reflectance spectra than the other widely used AC processors, i.e., C2RCC (a SNAP plugin). As ACOLITE processor is image-based, it does not require any *in-situ* measurements. By default, ACOLITE performs AC using the 'dark spectrum fitting' (DSF) algorithm for aerosol corrections. However, this algorithm avoids severe glints for which the glint effects can still be found in the DSF-derived surface reflectance<sup>44</sup>. As sun glint was a prominent optical phenomenon in the study region, especially during spring and summertime, the optional glint correction within ACOLITE was also applied. The land and clouds were masked during the AC processing to retain the water-leaving reflectance. Therefore, the data were inspected visually. In some cases where high clouds (i.e. cirrus, cirrostratus, and cirrocumulus) and haze were left unmasked, and when these were found to degrade the region of interest near the coast, the images were discarded.



Occasionally, images with clear meteorological conditions were also discarded after visual inspection due to significant turbidity being visible in the shallow waters. This was done as it significantly affected the colour of the water and made it impossible to observe through the water column. These strict criteria only admitted images that were of very good quality. To remove boats, very large waves, and other anomalies, as well as to reduce noisy patterns and artifacts to improve the overall quality of the image, a pixel-by-pixel median stacking was performed for the blue (B), green (G), and red (R) bands of all the good quality atmospherically processed data (3–9 images per year).

The EMODnet bathymetry data was reprojected and resampled to 10m (using the bilinear interpolation technique) to match the projection system and the spatial resolution of the Sentinel-2 data. The data was cropped after 40m depth to remove open and deep ocean pixels to avoid potential FP of *P. oceanica*, as both classes had similar spectral values<sup>36</sup>.

The marine habitats of the *in-situ* data were classified into two classes, i.e. "PO" (indicating the habitat of *P. oceanica*) and "Non-PO" (indicating other than the habitat of *P. oceanica*). *In-situ* data corresponding to land, offshore, and shallow water with a sandy/rocky habitat or other seagrass habitats were included in the Non-PO class. The PO and Non-PO classes were labelled as 1 and 0, respectively, and rasterized using the same projection system of Sentinel-2 scenes.

## Artificial intelligence-based DLNN approach

The identification of *P. oceanica* is a binary classification problem where pixels correspond to either PO or Non-PO. Therefore, the aim of using a DLNN model was to train a function based on the given satellite and bathymetry dataset (X) as well as target *in-situ* data (Y) to output a predicted class ( $\hat{Y}$ ) of PO and Non-PO, which should match as closely as possible with the *in-situ* data (Y).

The training was done through two processes, namely, forward propagation and backpropagation to recognize patterns based on the given dataset. In forward propagation, the process moved in the forward direction through the neural network (NN) to produce a final value at the output layer, whereas at the same time, in backpropagation, the process moved from the output layer to the input layer to improve the weight (w) value generated in the forward process. Forward propagation was a value-processing step from the input layer that involved calculating a linear combination per neuron using adjustable linear coefficients and then calculating an activation function by performing a non-linear transformation for the corresponding neuron within the layers. The activation functions of all the layers except the last one were simply rectified linear unit activations, meaning that the output was set to zero if it was negative. Hence, the output coefficients from the neurons never had negative values. In the DLNN model, the last layer was a binary classifier, which means that it classified pixels as belonging to either class 1 or class 0. In this case, the activation function was a sigmoid function, which predicted the probability ( $\hat{Y}$ ) of a pixel being class 1 or 0 based on a threshold value of 0.5.

To optimize the training process, we performed mini-batch processing, where we split the training set into smaller sets and implemented gradient descent on each batch chronologically to make the algorithm

work faster. Therefore, based on the input data, each 10m pixel of the Sentinel-2 image was classified as containing PO (class 1) or Non-PO (class 0). The result,  $\hat{Y}$ , was compared to  $Y$ , and the difference was quantified in a cost function. Minimizing the cost function equates to making  $\hat{Y}$  as similar as possible to  $Y$ . The differences between  $\hat{Y}$  and  $Y$  per pixel allowed the calculation of the gradient that quantified how much each coefficient in each neuron must be altered to match  $\hat{Y}$  to  $Y$ . This gradient was then used to update the coefficients in the neurons of all the layers through backpropagation. This was an iterative process, and therefore, at each iteration, a new prediction was made, compared to the target  $Y$ , a gradient was calculated, and the coefficients were updated. This process was carried out continuously until it produced the smallest loss value, and the output was saved in the form of a file containing the weight ( $w$ ) and bias ( $b$ ) values. Afterward, the derived set of coefficients from the DLNN model was used to map *P. oceanica*.

## Post-processing and accuracy assessment

In the post-processing step, we evaluated several filters, i.e. sieve (replacing small isolated groups of pixels with the pixel value of the largest neighbour), median (ranking values of the pixels in the moving window with a specified radius and taking the middle-ranking value), bilateral (replacing the value of each pixel with a weighted average of the pixel values in the moving window), and principal component analysis (removing noise by discarding the last principal components that explain the least of variance). Among them, we chose the median filter with 3x3 pixels moving window as it significantly reduced the noise while preserving the shape of the seagrass patches. We applied the filter to the binary maps and merged the resultant maps per region to produce the regional map. Then we calculated the overall, producer's, and user's accuracies of the final map using the corresponding geo-referenced *in-situ* data. The overall accuracy expressed the ratio of the number of correctly classified pixels to the total number of given pixels regardless of the class. Producer's accuracy expressed how often *P. oceanica* could be identified correctly on the classified map; whereas, the user's accuracy expressed how often the *P. oceanica* class on the map would be present on the ground. Producer's accuracy is the map accuracy from the mapmaker's viewpoint and so it is a great statistical metric for the remote sensing scientist creating the habitat map. In contrast, the user's accuracy is the accuracy from the map user's viewpoint. Hence, it is more significant in a management context of a given region as it reports a quantitative probability for the actual presence of the studied habitat (in this case, *P. oceanica*) in the given region<sup>37</sup>. The equations for all the aforementioned classification metrics are given below:

$$\text{Overall accuracy} = \frac{TP+TN}{n} \text{ (Eq. 1)}$$

$$\text{Producer's accuracy} = \frac{TP}{TP+FN} \text{ (Eq. 2)}$$

$$\text{User's accuracy} = \frac{TP}{TP+FP} \text{ (Eq. 3)}$$

Here, TP is the number of true positives, i.e., pixels correctly identified as PO; TN is the number of true negatives, i.e., pixels correctly identified as Non-PO; FP is the number of false positives, i.e., the number of

actual Non-PO pixels classified as PO; and FN is the number of false negatives, i.e., the number of actual PO pixels classified as Non-PO.

## Declarations

## Acknowledgements

This study is a part of SIMBAD project (QSR-ESABIC-2018-001) incubated by the European Space Agency Business Incubation Centre (ESA-BIC) Madrid Region, which facilitates incentives for business projects and start-ups to use space technologies or to develop applications based on these technologies with the aim of developing new products and services unrelated to space. The authors are thankful to the support from the Parque Científico de Madrid where Quasar Science Resources, S.L. is incubated. The first author is supported by the Industrial Doctorate Program of the Spanish Ministerio de Ciencia e Innovación (ref. DIN2020-010979/AEI/10.13039/501100011033). This work is part of the first author's PhD within the SIMBAD project. The authors would like to thank the rest of the SIMBAD team. The authors are thankful to the European Space Agency, the European Commission, and the Copernicus programme for distributing Sentinel-2 imagery. This research would not be possible without the *in-situ* data kindly provided by ERA and Gobierno Balear. The *in-situ* data for the Maltese Islands was collected within the scope of the Marine Environmental Monitoring: Towards Effective Management of Malta's Marine Waters project (ERA 2017). Details on the survey performed can be found in Dewey and MacMillan (2021). We would like to thank Marcial Bardolet Richter (Técnico de IBANAT. Consellería de Medi Ambient i Territori), from D.G. Biodiversidad y Espacios Naturales, Consellería de Medi Ambient i Territori de les Illes Balears, Govern Balear, for providing the *in-situ* data for the Balearic Islands region.

## Authors' contributions

MC, AM, MM, NB, IC, MR and IdC contributed with ideas to design the research objectives. AM led the design of the architecture of the scientific modules. MC and AM developed the scientific modules for data pre-processing, the DLNN model and its accuracy assessment, whereas NB developed the filters and time-series analysis, with support from IdC. EP and JB contributed to the SEP's development. MM conducted all the model runs within the Docker environment for the operational approach, with support from EP. MC wrote the original manuscript with input from MM. All authors contributed to the interpretation and discussion of results and the final manuscript. IdC and JB provided part of the financial support leading to this publication.

## Data Availability

The necessary procedures to generate the data and reproduce the methodology have been outlined in the manuscript. The data that support the findings of this study are available from the authors on reasonable request.

# Competing Interest

The author(s) declare no competing interests.

## References

1. McKenzie, L. J. *et al.* The global distribution of seagrass meadows. *Environ. Res. Lett.* 15, 074041 (2020).
2. Duarte, C. M. *et al.* Seagrass community metabolism: Assessing the carbon sink capacity of seagrass meadows. *Glob. Biogeochem. Cycles* 24, (2010).
3. Short, F. T. *World Atlas of Seagrasses*. (University of California Press, 2003).
4. de los Santos, C. B. *et al.* Recent trend reversal for declining European seagrass meadows. *Nat. Commun.* 10, 3356 (2019).
5. Waycott, M. *et al.* Accelerating loss of seagrasses across the globe threatens coastal ecosystems. *Proc. Natl. Acad. Sci.* 106, 12377–12381 (2009).
6. Marbà, N., Díaz-Almela, E. & Duarte, C. M. Mediterranean seagrass (*Posidonia oceanica*) loss between 1842 and 2009. *Biol. Conserv.* 176, 183–190 (2014).
7. Ibiza News. *Posidonia Will Disappear From Ibiza And Formentera If Sea Temperatures Continue To Rise.* *Ibiza News* <https://www.diariodeibiza.com/ibiza/posidonia-sea-temperatures-rise/> (2023).
8. MPN. Mediterranean Posidonia Network. *Mediterranean Posidonia Network* <https://medposidonianetwork.com/> (2023).
9. Bethoux, J. & Copin Montegut, G. BIOLOGICAL FIXATION OF ATMOSPHERIC NITROGEN IN THE MEDITERRANEAN-SEA. *Limnol. Oceanogr.* 31, 1353–1358 (1986).
10. MedWet. *Posidonia, the lung of the Mediterranean* | MedWet. <https://medwet.org/2017/10/mediterranean-posidonia/> (2017).
11. Calvo, S., Ciraolo, G. & Loggia, G. L. Monitoring *Posidonia oceanica* meadows in a Mediterranean coastal lagoon (Stagnone, Italy) by means of neural network and ISODATA classification methods. *Int. J. Remote Sens.* 24, 2703–2716 (2003).
12. Francour, P. Fish Assemblages of *Posidonia oceanica* Beds at Port-Cros (France, NW Mediterranean): Assessment of Composition and Long-Term Fluctuations by Visual Census. *Mar. Ecol.* 18, 157–173 (1997).
13. Hemminga, M. A. & Duarte, C. M. *Seagrass Ecology*. (Cambridge University Press, 2000).
14. Gacia, E., Granata, T. C. & Duarte, C. M. An approach to measurement of particle flux and sediment retention within seagrass (*Posidonia oceanica*) meadows. *Aquat. Bot.* 65, 255 (1999).
15. Fourqurean, J. W. *et al.* Seagrass ecosystems as a globally significant carbon stock. *Nat. Geosci.* 5, 505–509 (2012).
16. IUCN. Manual for the Creation of Blue Carbon Projects in Europe and the Mediterranean. at <https://iucn.org/resources/file/manual-creation-blue-carbon-projects-europe-and-mediterranean>

(2021).

17. Duarte, C. M., Losada, I. J., Hendriks, I. E., Mazarrasa, I. & Marbà, N. The role of coastal plant communities for climate change mitigation and adaptation. *Nat. Clim. Change* 3, 961–968 (2013).
18. Arias-Ortiz, A. *et al.* A marine heatwave drives massive losses from the world's largest seagrass carbon stocks. *Nat. Clim. Change* 8, 338–344 (2018).
19. Jordà, G., Marbà, N. & Duarte, C. M. Mediterranean seagrass vulnerable to regional climate warming. *Nat. Clim. Change* 2, 821–824 (2012).
20. Wernberg, T. *et al.* An extreme climatic event alters marine ecosystem structure in a global biodiversity hotspot. *Nat. Clim. Change* 3, 78–82 (2013).
21. EEA. Grouped threats to *Posidonia oceanica* beds as reported by Mediterranean EU Member States under the EU Habitats Directive – European Environment Agency. <https://www.eea.europa.eu/data-and-maps/figures/grouped-threats-to-posidonia-oceanica> (2015).
22. Mateo, M. A., Romeo, J., Perez, M., Littler, M. M. & Littler, D. S. Dynamics of millenary organic deposits resulting from the growth of the Mediterranean seagrass < I > *Posidonia oceanica*.</I>. (1997).
23. Lee, K.-S., Park, S. & Kim, Y. Effects of irradiance, temperature, and nutrients on growth dynamics of seagrasses: A review. *J. Exp. Mar. Biol. Ecol. - J EXP MAR BIOL ECOL* 350, 144–175 (2007).
24. Collado-Vides, L., Caccia, V. G., Boyer, J. N. & Fourqurean, J. W. Tropical seagrass-associated macroalgae distributions and trends relative to water quality. *Estuar. Coast. Shelf Sci.* 73, 680–694 (2007).
25. Duarte, C. M. The future of seagrass meadows. *Environ. Conserv.* 29, 192–206 (2002).
26. Short, F., Carruthers, T., Dennison, W. & Waycott, M. Global seagrass distribution and diversity: A bioregional model. *J. Exp. Mar. Biol. Ecol.* 350, 3–20 (2007).
27. Kenworthy, W., Wyllie-Echeverria, S., Coles, R., Pergent, G. & Pergent-Martini, C. Seagrass conservation biology: an interdisciplinary science for protection of the seagrass biome. *Seagrasses Biol. Ecol. Conserv.* (2006).
28. Sagawa, T. *et al.* Using bottom surface reflectance to map coastal marine areas: a new application method for Lyzenga's model. *Int. J. Remote Sens.* 31, 3051–3064 (2010).
29. Borfecchia, F. *et al.* Landsat 8 OLI satellite data for mapping of the *Posidonia oceanica* and benthic habitats of coastal ecosystems. *Int. J. Remote Sens.* 40, 1548–1575 (2019).
30. Cozza, R. *et al.* Biomonitoring of *Posidonia oceanica* beds by a multiscale approach. *Aquat. Bot.* 156, 14–24 (2019).
31. Dattola, L. *et al.* Comparison of Sentinel-2 and Landsat-8 OLI satellite images vs. high spatial resolution images (MIVIS and WorldView-2) for mapping *Posidonia oceanica* meadows. in *Remote Sensing of the Ocean, Sea Ice, Coastal Waters, and Large Water Regions 2018* vol. 10784 252–262 (SPIE, 2018).
32. Fornes, A. *et al.* Mapping *Posidonia oceanica* from IKONOS. *ISPRS J. Photogramm. Remote Sens.* 60, 315–322 (2006).

33. Matarrese, R., Acquaro, M., Morea, A., Tijani, K. & Chiaradia, M. T. Applications of Remote Sensing Techniques for Mapping Posidonia Oceanica Meadows. in *IGARSS 2008–2008 IEEE International Geoscience and Remote Sensing Symposium* vol. 4 IV-906-IV–909 (2008).
34. Pasqualini, V., Pergent-Martini, C., Clabaut, P. & Pergent, G. Mapping of Posidonia oceanica using Aerial Photographs and Side Scan Sonar: Application off the Island of Corsica (France). *Estuar. Coast. Shelf Sci.* 47, 359–367 (1998).
35. Topouzelis, K., Makri, D., Stoupas, N., Papakonstantinou, A. & Katsanevakis, S. Seagrass mapping in Greek territorial waters using Landsat-8 satellite images. *Int. J. Appl. Earth Obs. Geoinformation* 67, 98–113 (2018).
36. Traganos, D. *et al.* Spatially Explicit Seagrass Extent Mapping Across the Entire Mediterranean. *Front. Mar. Sci.* 9, (2022).
37. Traganos, D. & Reinartz, P. Mapping Mediterranean seagrasses with Sentinel-2 imagery. *Mar. Pollut. Bull.* 134, 197–209 (2018).
38. Traganos, D. & Reinartz, P. Machine learning-based retrieval of benthic reflectance and Posidonia oceanica seagrass extent using a semi-analytical inversion of Sentinel-2 satellite data. *Int. J. Remote Sens.* 39, 9428–9452 (2018).
39. Poursanidis, D., Traganos, D., Reinartz, P. & Chrysoulakis, N. On the use of Sentinel-2 for coastal habitat mapping and satellite-derived bathymetry estimation using downscaled coastal aerosol band. *Int. J. Appl. Earth Obs. Geoinformation* 80, 58–70 (2019).
40. Colantoni, P., Galignani, P., Fresi, E. & Cinelli, F. Patterns of Posidonia oceanica (L.) Delile Beds around the Island of Ischia (Gulf of Naples) and in Adjacent Waters. *Mar. Ecol.* 3, 53–74 (1982).
41. Meinesz, A. & Laurent, R. Cartographie et état de la limite inférieure de l'herbier de Posidonia oceanica dans les Alpes-maritimes (France) – Campagne Poseidon 1976 —. *Bot. Mar.* 21, 513–526 (1978).
42. Boudouresque, C.-F., Blanfuné, A., Pergent, G. & Thibaut, T. Restoration of Seagrass Meadows in the Mediterranean Sea: A Critical Review of Effectiveness and Ethical Issues. *Water* 13, 1034 (2021).
43. Vanhellemont, Q. & Ruddick, K. Acolite for Sentinel-2: Aquatic Applications of MSI Imagery. (2016).
44. Vanhellemont, Q. & Ruddick, K. Atmospheric correction of metre-scale optical satellite data for inland and coastal water applications. *Remote Sens. Environ.* 216, 586–597 (2018).

## Figures

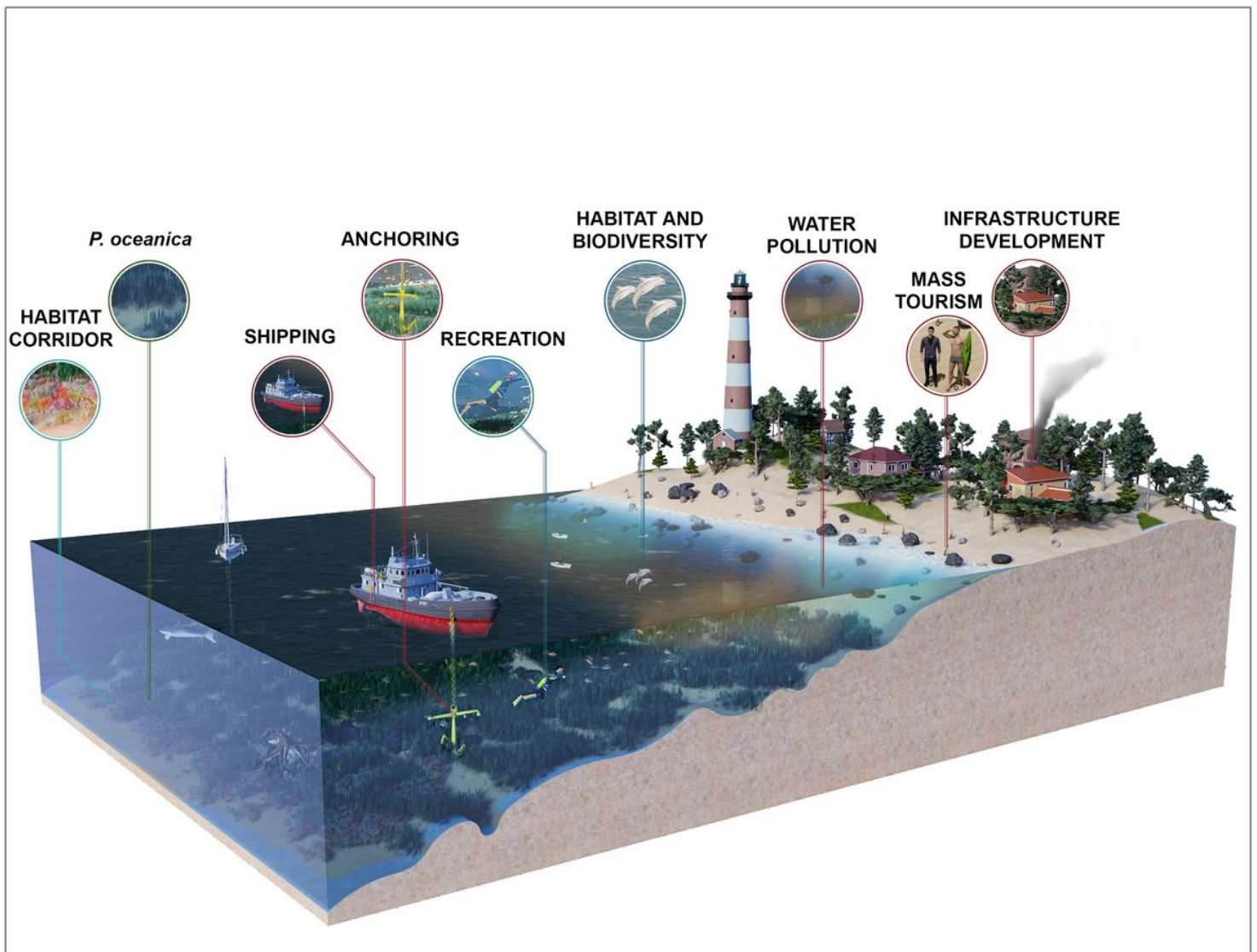


**Figure 1**

Why conservation of *P. oceanica* is important?

Conceptual diagram depicting the ecosystem services of *P. oceanica* (outlined by blue lines) and the anthropogenic pressures on the meadows (outlined by red lines). The meadows are endemic and dominant seagrass species in the Mediterranean Sea that controls its coastal and aquatic ecosystem. They provide shelter as well as act as a nursery for thousands of marine animals and plants, several of which are endangered species such as sea turtles and dugongs. The plant itself oxygenates the water and stabilizes the sandy shores and sea beds. They provide food directly through grazing or indirectly through detritus cycle<sup>9</sup>. They create ecological corridors between different habitats and are also globally significant carbon sinks<sup>13</sup>. The meadows are threatened by different anthropogenic activities, i.e. coastal infrastructure development, water pollution, fishing, shipping and anchoring. Over the last 50 years, the Mediterranean basin lost 13-50% of the areal extent of this meadow<sup>4</sup>. The recent warming of the Mediterranean Sea exaggerates the situation even more, which calls for continuous monitoring of the



meadows, identifying potential areas to mitigate the human impacts as well as selection of sites for conservation and restoration.

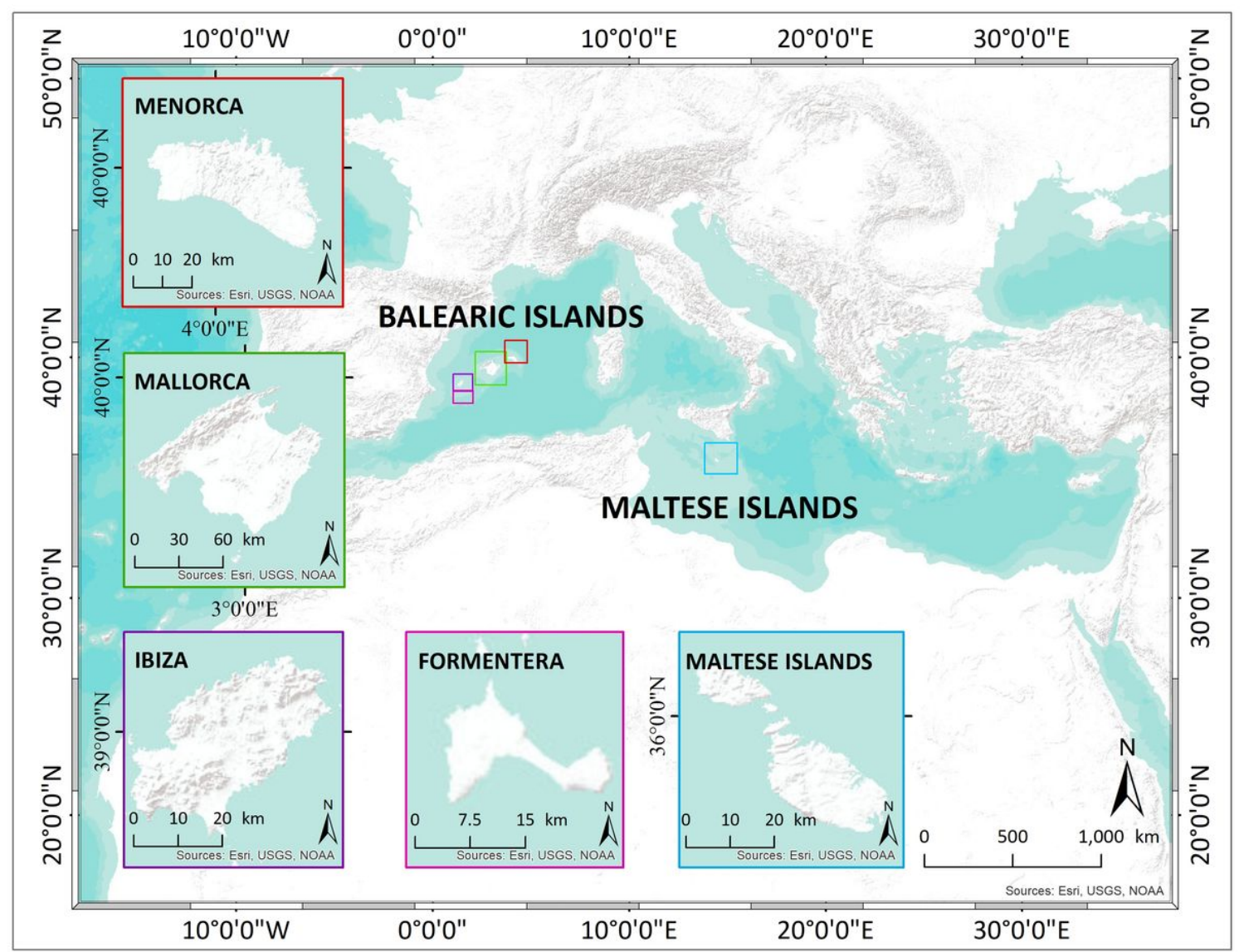


**Figure 2**

### Study regions

The study regions include four Islands, namely Menorca, Mallorca, Ibiza and Formentera from the Balearic Islands in Spain, and the Maltese Islands located in the western and the central Mediterranean Sea, respectively. The continental shelf of the Balearic Islands is nearly horizontal and situated at 93m depth on an average. The coastal waters are highly transparent due to the absence of rivers and the infiltration of rainfall in the karstic soils. Currently, 73% of the Balearic coastline is under protection through the Natural Areas of Special Interest, National Natural Park, Natura2000 sites, and the UNESCO Biosphere Reserve. In contrast, the Maltese Islands consist of shallow water, and the surrounding seafloor comprises an irregularly shaped continental shelf. Sandy bottoms with *P. oceanica* and *C. nodosa*



characterize the dominant benthic habitats in shallow waters, mainly the offshore east coast of the Maltese archipelago.

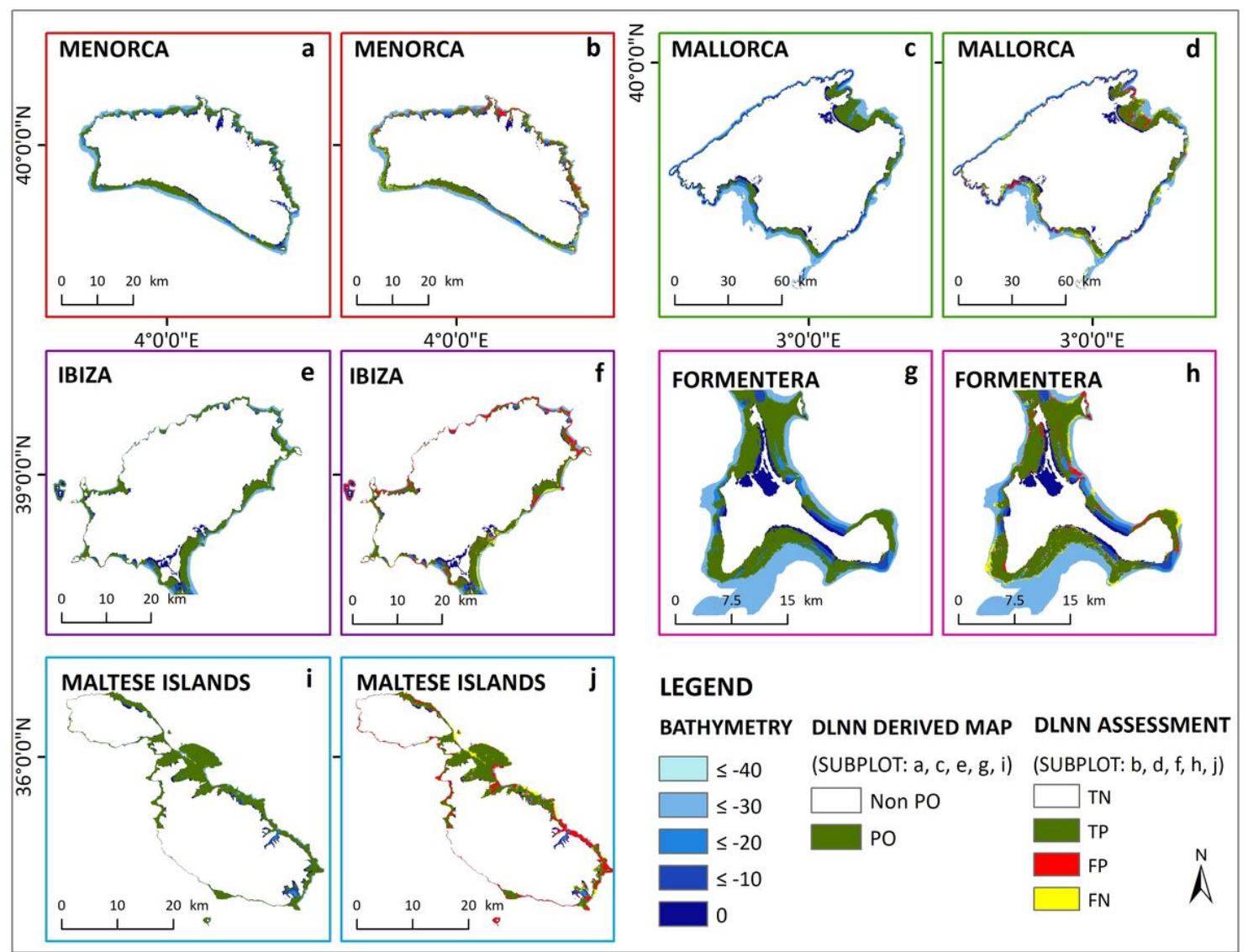


**Figure 3**

Regional maps of *P. oceanica* meadows

Regional maps of *P. oceanica* obtained through training the DLNN model with the corresponding in-situ data for the Balearic and Maltese Islands. The maps have 10m spatial resolution. Each pixel was identified as either PO or Non PO by the DLNN model. Subplots a, c, e, g, and i demonstrate the spatial extent of the meadows identified by the DLNN model in Menorca, Mallorca, Ibiza, Formentera, and the Maltese Islands, respectively. Subplots b, d, f, h, and j demonstrate model's performance per pixel for the corresponding regions. TN is True Negatives (pixels correctly identified as Non-PO), TP is True Positives (pixels correctly identified as PO), FP is False Positives (Non-PO pixels classified as PO), and FN is False Negatives (PO pixels classified as Non-PO).

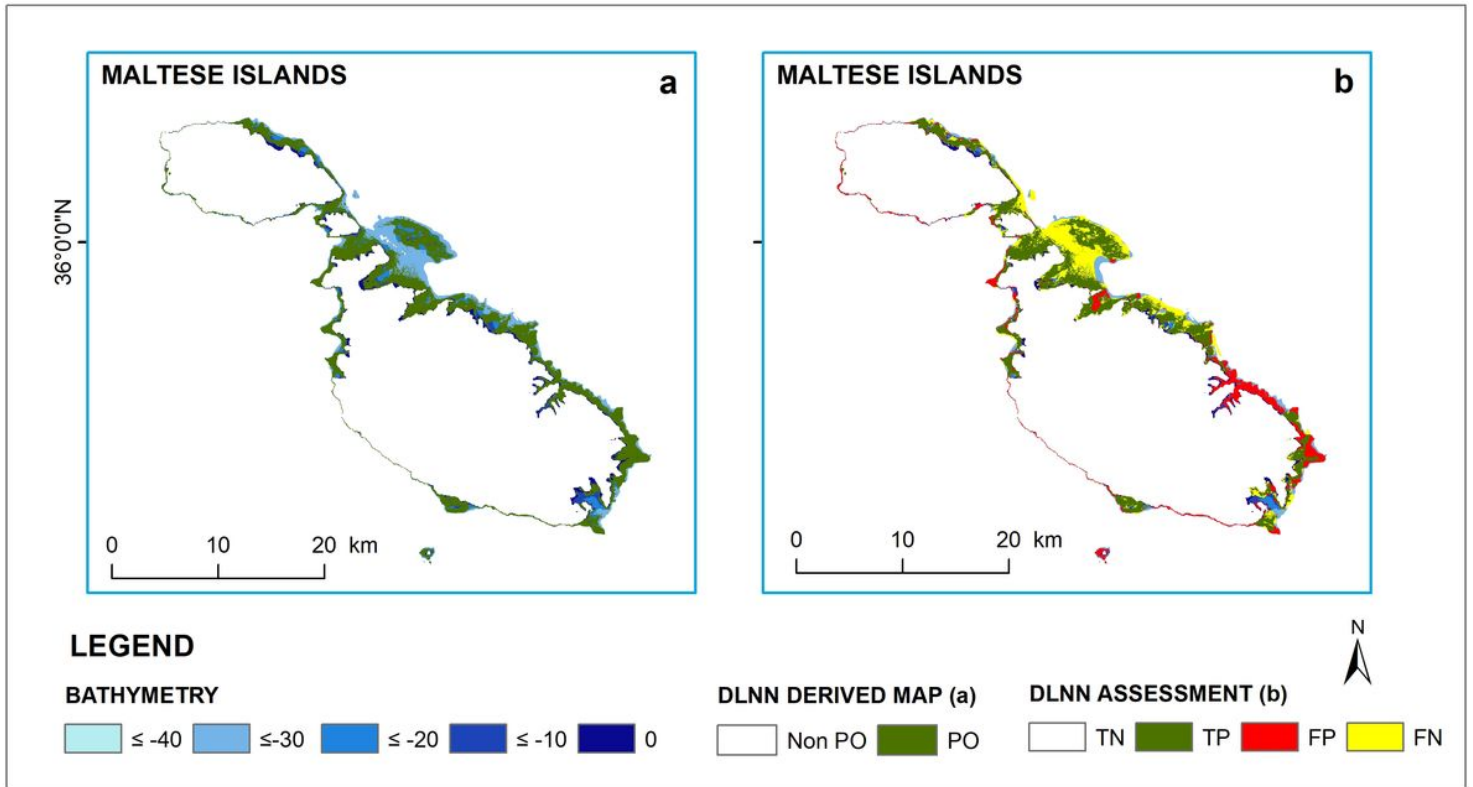


**Figure 4**

DLNN model trained with Formentera in-situ data

Map of *P. oceanica* in the Maltese Islands using the training dataset from Formentera. The maps have 10m spatial resolution. Each pixel was identified as either PO or Non PO by the DLNN model. Subplot a demonstrates the spatial extent of the meadows identified by the DLNN model, whereas subplot b demonstrates the model's performance per pixel for the Islands. TN is True Negatives (pixels correctly identified as Non-PO), TP is True Positives (pixels correctly identified as PO), FP is False Positives (Non-PO pixels classified as PO), and FN is False Negatives (PO pixels classified as Non-PO).

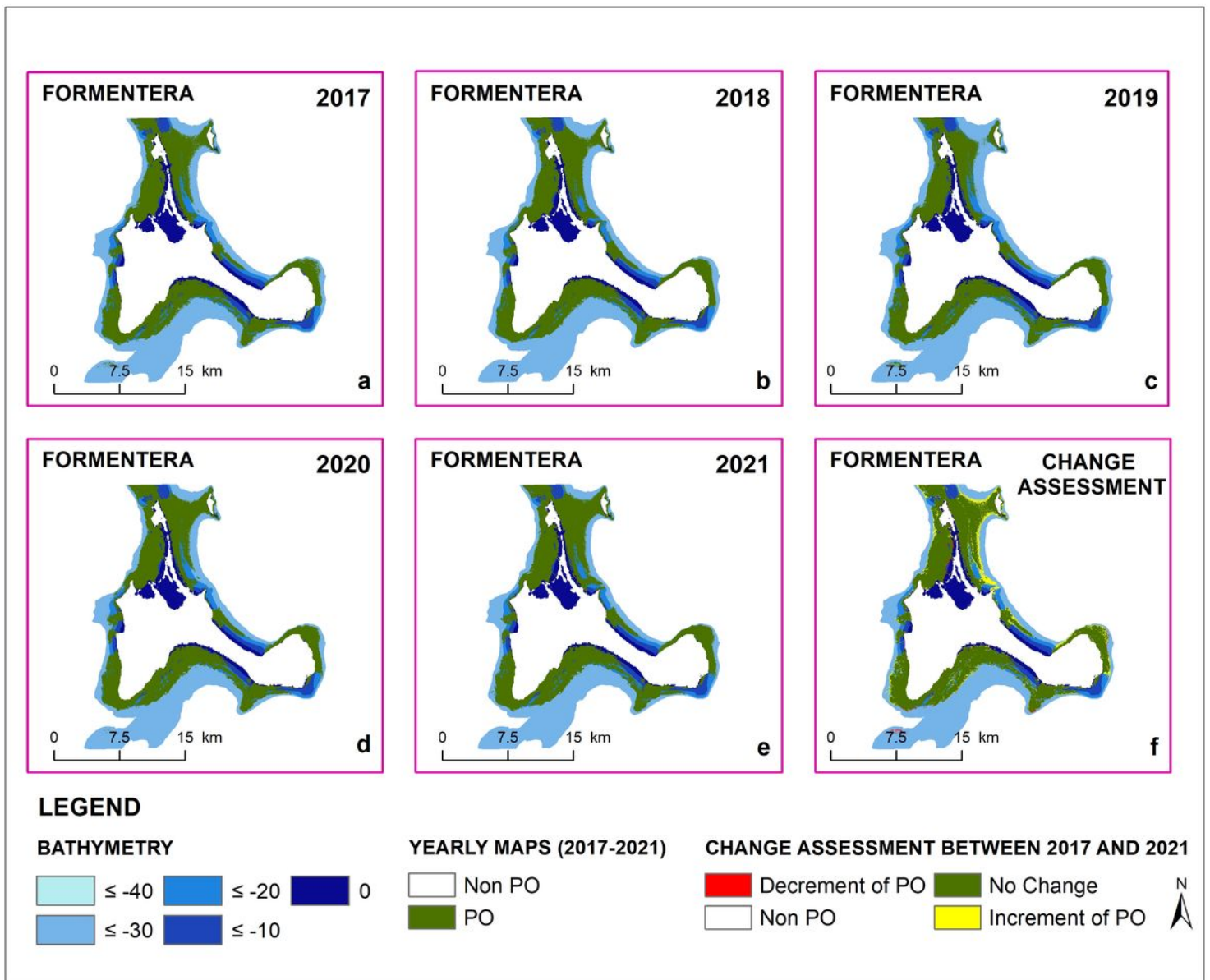


**Figure 5**

Yearly monitoring of *P. oceanica* and its change assessment

Yearly maps of *P. oceanica* in Formentera during 2017-2021. The seagrass patches mostly look stable during this period, except the northern part of the Island, where we detected a loss of the meadows until 2019 and then a subsequent gain since 2020.

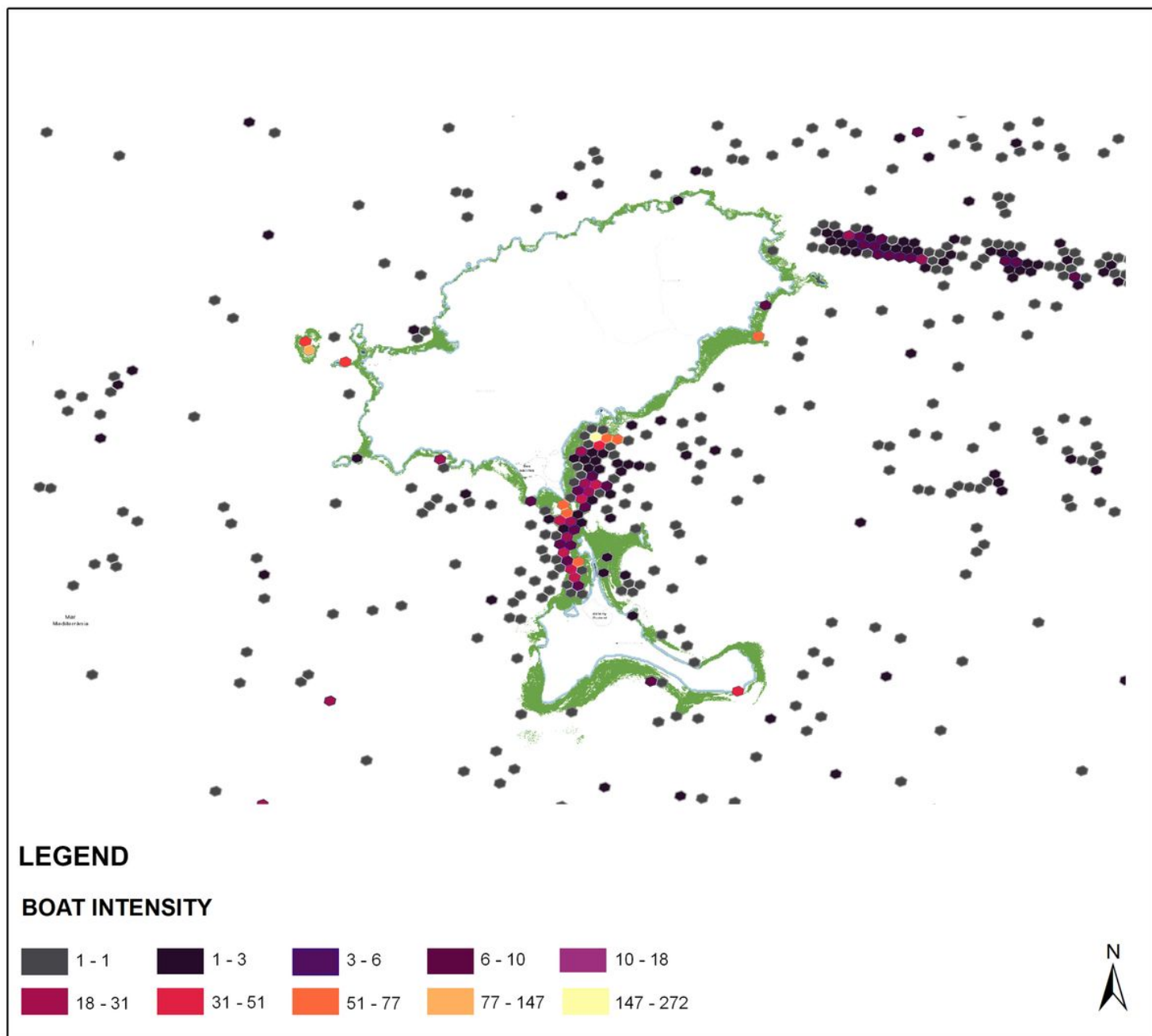


**Figure 6**

Boat intensity over the *P. oceanica* meadows

Boat pressure over the meadows in Formentera and Ibiza during June-August 2021, a peak tourist season. Each hexagon mesh presents the number of ships detected through Sentinel-1 satellite.

## Supplementary Files

This is a list of supplementary files associated with this preprint. Click to download.

- [Supplementarymaterials.pdf](#)